Available online at www.sciencedirect.com
SCIENCE DIRECT®
Journal of Colloid and Interface Science 273 (2004) 478–482
JOURNAL OF Colloid and Interface Science
www.elsevier.com/locate/jcis

ZnS/CdS/ZnS quantum dot quantum well produced in inverted micelles

Lixin Cao,[a,b,*] Shihua Huang,[a] and Shulin E [a]

[a] *Laboratory of Excited State Processes and Changchun Institute of Optical, Fine Mechanics and Physics, Chinese Academy of Sciences, Changchun 130021, People's Republic of China*

[b] *Institute of Materials Sciences and Engineering, Ocean University of China, Qingdao 266003, People's Republic of China*

Received 16 July 2003; accepted 6 February 2004

Abstract

A ZnS/CdS/ZnS quantum dot quantum well was prepared in AOT micelles successfully and was characterized by absorption spectroscopy and fluorescence spectroscopy. Luminescence in the region of 350–600 nm was observed. The complete ZnS shell might reduce the number of defects on the surface of the CdS well, which were assumed to act as centers for radiationless recombination, resulting in the luminescence enhancement.

Keywords: Quantum dot quantum well; ZnS; CdS

1. Introduction

Semiconductor nanomaterials, as a new type of luminescent material, have drawn considerable interest in recent years [1–5]. Quantum confinement effect and surface effect are the two key factors determining the optical properties of the nanoparticles. Surface states usually act as the radiationless recombination centers. So the surface modification of nanoparticles which could passivate the surface becomes an active research field [6–12]. The first approach to modification is capping the nanoparticles with some organic molecule. Although this method cannot passivate the surface perfectly, the quantum yield has reached about 10% at room temperature [6,7]. The second method is to attempt to grow a second semiconductor material on the surface of a given nanoparticle. The quantum yield at room temperature has been raised to about 20% by this method [12]. In recent years, a new method has been developed by Weller and his collaborators [13–15]. They prepared the first three-layered compound which consists of a core of size-quantized CdS coated with a layer of HgS as the well, which itself was covered by, again, CdS as the outermost shell. They called this structure quantum dot quantum well (QDQW). The electronic properties of QDQW may be controlled by tuning the thickness and the energetic structures of various layers. A luminescence with high efficiency may be obtained. ZnS has the cubic structure of a blende type ($a = 5.406$ Å), very close to that of CdS ($a = 5.818$ Å), and a large gap (3.7 eV) compared to the gap of CdS (2.5 eV) [16]. There are basic conditions for forming a QDQW structure with ZnS and CdS. In this paper, ZnS/CdS/ZnS QDQW was prepared and characterized. The QDQW's optical properties were not just the superposition of those of separated ZnS and CdS nanoparticles. The luminescence was enhanced by the complete ZnS shell.

2. Experimental methods

All solvents and chemicals were analytical reagent grade and were used as received. AOT (dioctylsulfosuccinate sodium salt) was dissolved in heptane at a concentration of 4×10^{-2} M. Standard solutions of Zn^{2+} (0.206 and 1.375 M) and Cd^{2+} (0.200 M) were prepared from $Zn(NO_3)_2$, $Cd(NO_3)_2$, and purified water.

2.1. Formation of colloidal ZnS core

Eight hundred milliliters of 0.04 M AOT heptane solution was mixed with 2.3 ml 0.206 M $Zn(NO_3)_2$ aqueous. The mixture was stirred magnetically until the mixture became homogeneous. This preparation gave a microemulsion with the water-to-surfactant mole ratio $W = 4$. The microemul-

* Corresponding author.
E-mail address: 9990629@sina.com (L. Cao).

0021-9797/$ – see front matter
doi:10.1016/j.jcis.2004.02.031

sion was bubbled with N_2 gas for 30 min before excess H_2S was introduced. Finally, the nonreacted H_2S was blown out by N_2 and the ZnS core in AOT in heptane was obtained.

2.2. Deposition of a CdS well on the surface of the ZnS core

The calculated amount of 0.2 M $Cd(NO_3)_2$ aqueous solution was added to the ZnS core colloidal solution and stirred magnetically for 20 min. Thus the nanoparticles with a ZnS core covered by a CdS well in AOT in heptane were obtained. The thickness of the CdS well can be controlled by changing the amount of added $Cd(NO_3)_2$ aqueous solution.

2.3. Deposition of incomplete ZnS shell on the surface of CdS well

Excess H_2S was divided into several parts and injected into ZnS core–CdS well colloidal solution at intervals of 20 min. After the reaction was complete, the unreacted H_2S was removed by bubbling N_2 gas through the solution for at least 30 min. In this step, an incomplete shell of ZnS was deposited on the surface of a CdS well.

2.4. Thickening of CdS well and deposition of complete ZnS shell

Repeating procedures 2 and 3 resulted in the CdS well thickening and an incomplete ZnS shell depositing. Then, another appropriate amount of $Zn(NO_3)_2$ was added to this solution drop by drop, with the injection of H_2S continuing in the meantime. After reaction, the removal of excess H_2S by N_2 gas bubbling led to the formation of a complete shell of ZnS. The thickness of the ZnS shell can be controlled by changing the amount of added $Zn(NO_3)_2$ aqueous solution. In this step, the concentrations of Zn^{2+} and S^{2-} ions remained very low during the reaction.

A ICP-AES/MS spectrometer (TJA POEMS) was used to measure the ion concentrations. X-ray photoelectron spectroscopy (XPS) measurements were performed using an Escalab MARK II spectrometer. Absorption spectra were measured with a Shimadzu recording spectrophotometer. Fluorescence spectra were taken using a Hitachi F-4500 fluorescence spectrophotometer. Fluorescence quantum yields were determined by comparison with fluorescein in methanol, which is known to fluoresce with quantum yields of 1.

3. Results and discussion

The semiconductor particles are assumed to have grown to approximately the same size as the water pools of the reverse micelles in which they are prepared [8,17]. The size of the water pools can be estimated roughly by the water-to-surfactant mole ratio. A more precise relationship between W and the radius of the micelle water pool (r) is given in Eq. (1):

$$\left[(r+15)/r\right]^3 - 1 = 27.5/W. \tag{1}$$

In our experiment, the ZnS core was prepared at $W = 4$. Thus the radius of the ZnS core was estimated to be 1.5 nm. In this article, AOT was used as a microreactor which controlled the size of the nanoparticles. Because the high AOT concentrations interfere with the microscopy of the particles, the particles' transmission electron microscopic images were not obtained. The size of the ZnS nanoparticles was also calculated from the absorption spectrum (Fig. 1, spectrum 1) using the effective mass model of Brus. For ZnS, the effective masses of the electron and the hole were 0.42 and 0.61 m_e, respectively. The dielectric constant was 8.0. Then the radius of the ZnS nanoparticles was calculated to be 1.6 nm, which was consistent with the values estimated by W (1.5 nm). Since the solubility of the CdS product is at least 5 orders of magnitude smaller than that of ZnS, it is chemically reasonable to assume a substitution reaction,

$$(ZnS)_n + mCd^{2+} \rightarrow (ZnS)_{n-m}(CdS)_m + mZn^{2+},$$

taking place. Because of the absence of excess S^{2-} ions in the solution, the separated CdS single nanoparticles could not be formed directly. At first, Cd^{2+} ion was attached to the surface of ZnS nanoparticles, and then the Cd^{2+} ion displaced the Zn^{2+} ion in the Zn–S bond to form a Cd–S bond on the surface of ZnS nanoparticles. When all of the Zn^{2+} ions on the surface of the ZnS nanoparticles were replaced by Cd^{2+} ions, the reaction stopped. The amount of Cd^{2+} ions was excess so that the CdS layer could be complete. So there were excess Cd^{2+} ions present in the solution. The concentrations of Zn^{2+} and Cd^{2+} ions in the solutions of sample 1 and sample 3 were measured by ICP-AES/MS spectrometer. Since in 3-nm ZnS particles the surface-to-volume ratio is approximately 0.525, the concentrations of Zn^{2+} and Cd^{2+} ions before and after the substitution reaction can be estimated also by calculation according to the initial concentrations. The data are presented in Table 1.

The data in Table 1 confirm that the ion exchange reaction happened indeed. Subsequent slow introduction of H_2S first led to the excess Cd^{2+} ions converting to CdS and then led to the replaced Zn^{2+} ions converting to ZnS, forming an incomplete shell on the CdS layer because the replaced Zn^{2+} ions cannot completely cover the surface of the enlarged particles again. Another introduction of Zn^{2+} ions and H_2S resulted in the completion and thickening of the shell. Due to

Table 1
The concentrations of Zn^{2+} and Cd^{2+} ions

Sample	Concentration of Zn^{2+} (M)		Concentration of Cd^{2+} (M)	
	Calculated	Measured	Calculated	Measured
1	≈ 0	0.08×10^{-4}	0	
3	3.11×10^{-4}	2.93×10^{-4}	0.59×10^{-4}	0.71×10^{-4}
Initial	5.92×10^{-4}		3.70×10^{-4}	

Table 2
Some parameters and data of the samples

No.	Composition	Total amounts of $Cd(NO_3)_2$ and $Zn(NO_3)_2$	Comments	Molar ratio of Zn^{2+} to Cd^{2+}
1	ZnS core	2.3 ml 0.206 M $Zn(NO_3)_2$		
2	ZnS core $CdS_{0.62}$	Sample 1 + 0.74 ml 0.200 M $Cd(NO_3)_2$	With 0.62 monolayer of CdS	3.2:1
3	ZnS core $CdS_{1.00}$	Sample 2 + 0.74 ml 0.200 M $Cd(NO_3)_2$	With 1.00 monolayer of CdS and excess Cd^{2+}	1.6:1
4	ZnS core $CdS_{1.15}ZnS_{0.93}$	Sample 3	With 1.15 monolayer of CdS and 0.93 monolayer of ZnS	1.6:1
5	ZnS core $CdS_{1.15}ZnS_{1.21}$	Sample 4 + 0.12 ml 1.375 M $Zn(NO_3)_2$	With 1.15 monolayer of CdS and 1.21 monolayer of ZnS	2.2:1
6	ZnS core $CdS_{5.00}ZnS_{3.00}$	Sample 1 + 20.48 ml 0.200 M $Cd(NO_3)_2$ + 40.21 ml 0.206 M $Zn(NO_3)_2$	With 5.00 monolayer of CdS and 3.00 monolayer of ZnS	

Table 3
The atomic ratio between Zn and Cd at different depths in sample 6

Ar^+ ion etching time (s)	0	30	90
Atomic ratio Zn:Cd	1.04	0.69	0.89

the very low concentrations of Zn^{2+} and S^{2-} ions, the possibility of forming ZnS single nanoparticles is very small. Our experiments were completed at room temperature. At so low a temperature, the formation of mixed crystals of $Zn_xCd_{1-x}S$ was hardly possible. And the emission peak for our samples 2 to 4 centered at 520 nm (Fig. 4), very different from that for $Zn_xCd_{1-x}S$ shifting with X [21]. So, most of the Zn^{2+} ions formed a ZnS shell on the surface of the CdS well. Assuming the radius of the ZnS core could be estimated by W, the thicknesses of the well and the shell layer were estimated by taking into account the mole volumes of CdS (29.88 $cm^3\,mol^{-1}$) and ZnS (23.83 $cm^3\,mol^{-1}$) and the initial amounts of Zn^{2+} ions. According to the calculation, the diameter of the CdS molecule was about 0.46 nm and the diameter of the ZnS molecule was about 0.42 nm, which was the thickness of one monolayer of CdS and one monolayer of ZnS. Some parameters and data of the obtained samples are given in Table 2. The data are available only for reference.

For sample 6, the nanoparticles were precipitated from the solutions by adding amounts of water into the system and dried at room temperature. The powder of sample 6 was pressed into foil and used for XPS measurements. XPS is a technique whose surface sensitivities lie in the range of 4–12 Å. It can be used to demonstrate layering. In this experiment, an Ar^+ ion etching technique was used to detect the changes in the composition distribution with the depth from the surface. The atomic ratio between Zn and Cd in the outermost surface layers of sample can be obtained by correcting the ratio of the Zn_{2p} and Cd_{2p} peak integrated areas. The obtained data are listed in Table 3. It can be seen that the atomic ratio Zn:Cd reduced to 0.69 from 1.04 after the surface was etched by Ar^+ ion beam for 30 s. But after the surface was etched for 90 s, the atomic ratio Zn:Cd rose to 0.89 again. The result demonstrated the three layers in some degree. If the sample was a mixture of two separated

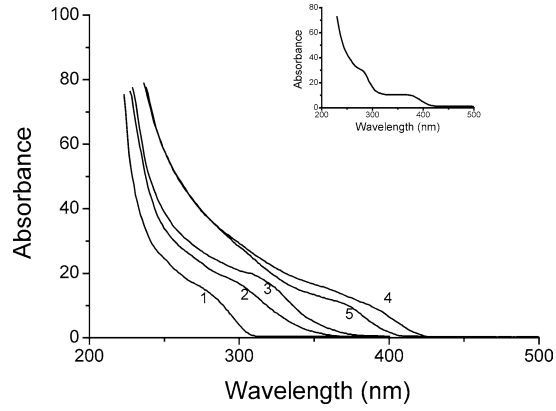

Fig. 1. Absorption spectra of the samples (the numbers 1, 2, 3, 4, 5 correspond to samples 1, 2, 3, 4, 5). Inset: Absorption spectrum of the mixture of ZnS colloidal solution and CdS colloidal solution with a Zn:Cd molar ratio of 1.6:1.

materials, the X-ray photoelectron spectra sampled over a relatively large area would show a uniform distribution of the composition into the mixture with the depth from the surface. The atomic ratio Zn:Cd would remain constant with the etching time.

The inset of Fig. 1 gives the absorption spectrum of the mixture of ZnS colloidal solution and CdS colloidal solution with a molar Zn:Cd ratio of 1.6:1. It can be seen that the absorption spectrum has two large shoulders at 280 and 380 nm attributed to the electron transition of size-quantized ZnS and CdS nanoparticles, respectively [18,19]. This is a characteristic of the superposition of the ZnS spectrum and the CdS spectrum.

Shown in Fig. 1 are the absorption spectra of the samples. For sample 1, an absorption onset at 300 nm and a large shoulder at 280 nm are observed. The shoulder is blue-shifted from 320 nm for the bulk ZnS because of quantum confinement. With the thickness of the CdS layer increasing, both the onset and the shoulder shifted to the red. For samples 1–3, the CdS layer increases from 0 monolayer to 1 monolayer, with the onset and the shoulder shifting to 355 and 325 nm from 300 and 280 nm, respectively. Subsequent sulfidation led to the red-shifting of the onset and the shoulder to 420 and 390 nm, respectively, in sample 4. The

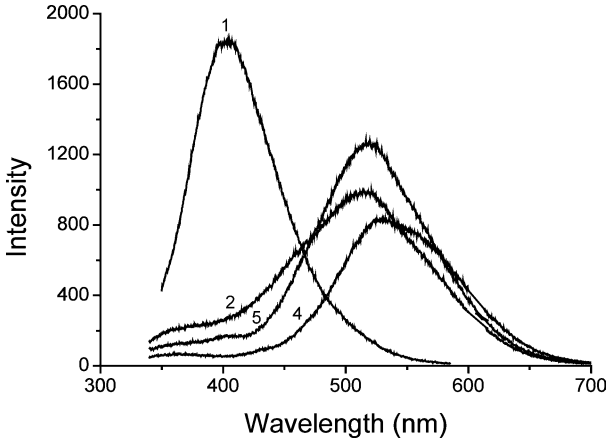

Fig. 2. Emission spectra of the samples excited at 298 (sample 1), 305 (sample 2), 305 (sample 4), and 308 nm (sample 5). (The numbers 1, 2, 4, 5 correspond to samples 1, 2, 4, 5.)

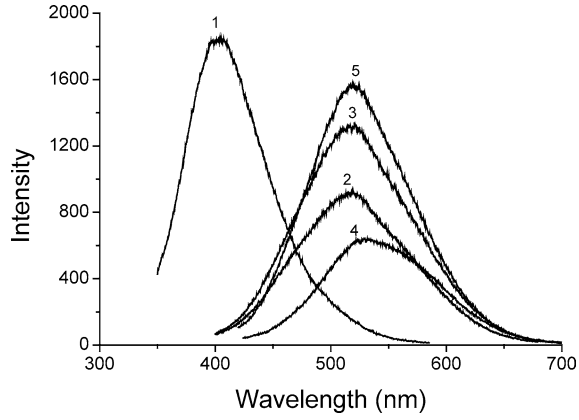

Fig. 3. Emission spectra of the samples excited with the most effective wavelength (sample 1, 298 nm; sample 2, 346 nm; sample 3, 346 nm; sample 4, 372 nm; sample 5, 371 nm). (The numbers 1, 2, 3, 4, 5 correspond to samples 1, 2, 3, 4, 5.)

red shift may be a result of the increased size of particles. The onset and the shoulder of sample 5 shifted to the blue slightly compared to sample 4. This indicates that sample 5 has fewer surface defects than sample 4. The absorption tail of sample 4 was assigned to the absorption of surface defects. Obviously, the spectra are not superpositions of the spectra of ZnS and CdS. These results indicate that there are interactions between ZnS and CdS. The regularity of the changes in the absorption spectra was consistent with that in the CdS/HgS/CdS system reported by Weller et al. [13], though the synthetic method was different.

Fig. 2 shows the emission spectra of the samples excited at the wavelength corresponding to the higher energy emission. It can be seen that the luminescence at 350–400 nm disappeared gradually with the CdS layer increasing to 1.15 monolayer and appeared again with the ZnS shell increasing. These phenomena confirmed the formation of the QDQW structure to some degree. Usually, the luminescence at 350–400 nm was attributed to the self-activated emission from ZnS [20]. The emission from the ZnS core was absorbed by the CdS well, which caused the gradual disappearance of this emission with the CdS well thickening. The emission from the ZnS shell resulted in the reappearance of this emission.

Presented in Fig. 3 are the emission spectra of samples excited with the most effective wavelength. A broad emission band for ZnS with maximum at 400 nm is observed in the spectrum of sample 1. This luminescence can be attributed to the self-activated emission caused by Zn vacancies in the lattice. With the CdS layer increasing from 0 monolayer to 1 monolayer, the luminescence maximum shifts from 400 to 520 nm and the luminescence intensity at 520 nm increases. When the 0.93 monolayer ZnS is capped on the surface of the CdS layer, the luminescence intensity reduces sharply. The increased interfaces introduced by the incomplete ZnS shell result in an increase in the radiationless paths. But after the ZnS shell is increased to 1.21 monolayer, the luminescence intensity rises again. Usually, the enhancement of the luminescence was attributed to the completion of the ZnS

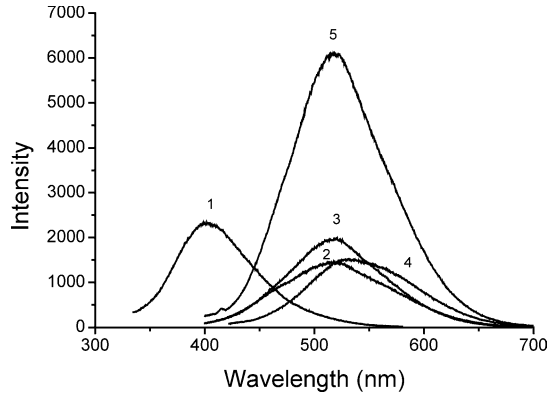

Fig. 4. Emission spectra of the samples 6 days after initial preparation excited with the most effective wavelength as for Fig. 3. (The numbers 1, 2, 3, 4, 5 correspond to samples 1, 2, 3, 4, 5.)

shell, which led to the number of radiationless centers being reduced [9,11].

Fig. 4 gives the emission spectra of the samples 6 days after initial preparation. It can be seen that the maximum position of the emission band of all the samples was unchanged, while the emission intensity increased to a different degree. Especially for sample 5, the emission intensity increased up to three times larger than that of the same sample just after the initial preparation.

The fluorescence quantum efficiency of samples 3 and 5, 6 days after initial preparation, was determined. The quantum yield was about 0.83% for sample 3 and 4.52% for sample 5. Although the quantum yield was still low, an increase in quantum efficiency of emission upon the ZnS shell was obtained.

It is reasonable to ask whether this luminescence enhancement and the increase in quantum yield of emission are caused by the size increase of the nanoparticles.

The absorption spectra of sample 5 just after and 6 days after the initial preparation were measured (Fig. 5). From the spectra, no change in the onset or the shoulder is ob-

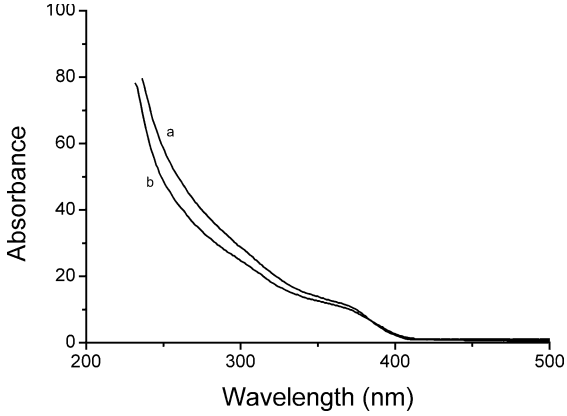

Fig. 5. Absorption spectra of sample 5 (a) just after and (b) 6 days after the initial preparation.

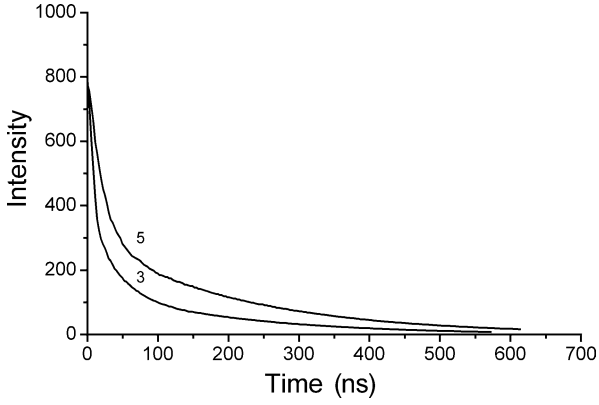

Fig. 6. Luminescence decay curves of sample 3 and sample 5 at 520 nm excited by 337 nm 6 days after the initial preparation.

served, while the absorbance changes slightly. Similar results were achieved for the other samples. These indicate that the nanoparticles did not grow. So the enhanced luminescence does not result from the nanoparticles' size increasing. We attribute the luminescence enhancement to two factors: one is the defective annealing and the other is the completion of the ZnS shell [9]. Both of the factors can lead to a decrease in the radiationless centers. The difference between our ZnS/CdS/ZnS QDQW and Weller's CdS/HgS/CdS QDQW [13] was that the ZnS shell only enhanced the luminescence from the CdS well in the ZnS/CdS/ZnS system, but the CdS shell led to the occurrence of a new fluorescent band in the CdS/HgS/CdS system.

Fig. 6 presents the luminescence decay curves of sample 3 and sample 5 at 520 nm excited by 337 nm 6 days after the initial preparation. It is shown that the luminescence decay of sample 5 was slower than that of sample 3. This indicates that the ZnS shell resulted in a luminescence decay slowdown. Usually the surface radiationless recombination would speed the luminescence decay. That the luminescence decay is slowed down indicates that some of the surface routes for radiationless recombination are blocked by the ZnS shell.

4. Conclusion

A ZnS/CdS/ZnS quantum dot quantum well was prepared in inverted micelles of AOT in heptane. The optical properties of the ZnS/CdS/ZnS QDQW were not just the superposition of the properties of separated ZnS and CdS nanoparticles. Luminescence in the region of 350–600 nm was observed. The luminescence from CdS was enhanced by the complete ZnS shell, which may be the result of the decrease in the defects on the surface of the CdS well, which were assumed to act as centers for radiationless recombination.

Acknowledgments

We thank the Natural Science Foundation of Shandong Province (Q2002B01), the Excellent Young Teachers Program of MDE, P.R.C. ([2003]355), and State Key Project of Basic Research (Grant 973.G19981309) for financial support.

References

[1] J.P. Kuczynski, B.H. Milosavljevic, J.K. Thomas, J. Phys. Chem. 88 (1984) 980.
[2] D.E. Dunstan, A. Hagfeldt, M. Almgren, H.O.G. Siegbahn, E. Mukhtar, J. Phys. Chem. 94 (1990) 6797.
[3] N. Murase, R. Jagannathan, Y. Kanematsu, M. Watanabe, A. Kurita, K. Hirata, T. Yazawa, T. Kushida, J. Phys. Chem. B 103 (1999) 754.
[4] U.H. Lee, D. Lee, H.G. Lee, S.K. Noh, J.Y. Leem, H.J. Lee, Appl. Phys. Lett. 74 (1999) 1597.
[5] A.V. Dijken, E.A. Meulenkamp, D. Vanmaekelbergh, A. Meijerink, J. Phys. Chem. B 104 (2000) 4355.
[6] C.B. Murray, D.J. Norris, M.G. Bawendi, J. Am. Chem. Soc. 115 (1993) 8706.
[7] D.J. Norris, A. Sacra, C.B. Murray, M.G. Bawendi, Phys. Rev. Lett. 72 (1994) 2612.
[8] C.F. Hoener, K.A. Allan, A.J. Bard, A. Campion, M.A. Fox, T.E. Mallouk, S.E. Webber, J.M. White, J. Phys. Chem. 96 (1992) 3812.
[9] A. Hässelbarth, A. Eychmüller, R. Eichberger, M. Giersig, A. Mews, H. Weller, J. Phys. Chem. 97 (1993) 5333.
[10] Y.C. Tian, T. Newton, N.A. Kotov, D.M. Guldi, J.H. Fendler, J. Phys. Chem. 100 (1996) 8927.
[11] B.O. Dabbousi, J.R. Viejo, F.V. Mikulec, J.R. Heine, H. Mattoussi, R. Ober, K.F. Jensen, M.G. Bawendi, J. Phys. Chem. B 101 (1997) 9463.
[12] L. Spahnel, M. Haase, H. Weller, A. Henglein, J. Am. Chem. Soc. 109 (1987) 5649.
[13] A. Eychmüller, A. Mews, H. Weller, Chem. Phys. Lett. 208 (1993) 59.
[14] A. Mews, A. Eychmüller, M. Giersig, D. Schooss, H. Weller, J. Phys. Chem. 98 (1994) 934.
[15] A.T. Yeh, G. Cerullo, U. Banin, A. Mews, A.P. Alivisatos, C.V. Shank, Phys. Rev. B 59 (1999) 4973.
[16] C. Ricolleau, L. Audinet, M. Gandais, T. Gacoin, Thin Solid Films 336 (1998) 213.
[17] P. Lianos, J.K. Thomas, Chem. Phys. Lett. 125 (1986) 299.
[18] H.C. Youn, S. Baral, J.H. Fendler, J. Phys. Chem. 92 (1988) 6320.
[19] K. Murakoshi, H. Hosokawa, S. Yanagida, Jpn. J. Appl. Phys. 38 (1999) 522.
[20] C.X. Liu, J.Y. Liu, W. Xu, Mater. Sci. Eng. B 75 (2000) 78.
[21] W.Z. Wang, I. Germanenko, M.S. El-Shall, Chem. Mater. 14 (2002) 3028.